



Combination of Gamma and X-ray Monte Carlo Simulation to Differentiate Between Uranium Oxide and Halides

M.H. Hazzaa^{1*}, S. E. Shaban¹, A. R. El Shahat¹, W. F. Khalil¹

¹Egyptian Nuclear and Radiological Regulatory Authority (ENRRA), P.O. Box 7551, Cairo, Egypt

*Corresponding author, Email address: Hazzaa_2012@yahoo.com

Received 10 March 2021,
Revised 10 April 2021,
Accepted 12 April 2021

Keywords

- ✓ HPGe detector ,
- ✓ MCNP-5,
- ✓ X-ray,
- ✓ Uranium.

Hazzaa_2012@yahoo.com
Phone: +201061840958

Abstract

Eleven samples were studied to differentiate between their chemical compositions using two different gamma detectors. Six samples were measured using Micro-trans-SPEC HPGe detector then underwent Monte Carlo simulation, MCNP code was used for calculating some nuclear parameters. It can be applied to calculate the absolute efficiency; hence, we can calculate the U-235 isotope mass by measuring count rate, the masses obtained by MCNP-5 were in a good agreement with the declared masses of the isotope U-235 with an average accuracy of about 1%, while the other five were simulated using MCNP-5 code. Count rates were calculated at different U-235 content. Electron beam interaction with samples was investigated, and characteristic X-ray was calculated with their spectrum. The X-ray was simulated using Si (Li) detector at 25 keV, probe dose 60.0 nA·s with no sample tilt and rotation. Combining results obtained from X-ray and gamma rays provides a clear view of differences between various uranium compounds. The proposed combination technique has proven to be extremely useful in the verification of nuclear safeguards. As a result, it is considered as a significant tool in nuclear inspections.

1. Introduction

Three methods, including relative, absolute and semi-absolute, are used to evaluate radioactive materials. Although the most precise results are commonly obtained using relative approaches, the key problem in this regard is the deficiency of radioactive material standards. Absolute or semi-absolute methods are considered if radioactive standards are not available or if the characteristics of the assayed materials differ from those of the standards. Factors, as well as parameters that affect measurements, have to be decided in this situation. The type and number of factors and parameters needed to test a radioactive material depend primarily on activity's purpose. When the objective is devoted to characterizing the material under investigation, all relevant factors influencing it must be determined. In both cases, the most important and difficult information to obtain is the detailed detector characteristics. Usually, information on detector design is provided by manufacturer. Nevertheless, this information is usually insufficient for allowing accurate modeling. As a result, and prior to starting modeling, extensive efforts should be made to ensure that detector is accurately characterized.

Several years ago, simulations of gamma-ray radiation detectors began utilizing MC calculations [1-3]. Several researchers frequently keep in mind various factors and complications that affect simulation.

For instance, this comprises simulation of detectors for generating calibration equations [4], computing efficiency and coincidence summing corrections [5], calculations in diverse energy ranges [6, 7], type of detector [8, 9], geometry factors, as well as other applications. Among all of the factors [10] and other applications [11-12].

In safeguard measurements, overcoming the distortion that occurs in the processing of fuel plates in Material Testing Reactor type (MTR) type fuel is a significant challenge. To reduce defects caused by chemical mixing in U₃O₈-Al Compact, a technique is provided that uses a mathematical model and MCNP code. The instrument in use is a High-Purity Germanium detector (HPGe). The model's and MCNP-5's results complement each other and are validated by comparison with declared values. The method could be useful in safeguards and Quality Control (QC) processes at the Fuel Manufacturing Pilot Plant (FMPP) [13].

Electrons accelerated to the material result in several interactions with atoms of target sample. The accelerated electrons can pass through sample with no interaction and can be elastically or inelastically dispersed. Both elastic as well as inelastic scattering lead to several signals utilized toward imaging, quantitative and semi-quantitative in formation of target sample, and X-ray source production. Imaging signals typically comprise secondary electrons (SE), backscattered electrons (BSE), cathode luminescence (CL), auger electrons as well as characteristic X-rays. Quantitative and semi-quantitative analysis of materials in addition to element mapping usually use characteristic X-rays. Bremsstrahlung (continuum) represents a continuous X-ray spectrum from zero to electron beam energy, forming a background with characteristic X-rays that should be taken into account. Furthermore, the X-rays produced by a particular target material are utilized as an approximately fixed-wavelength energy source amenable to be investigated using X-ray diffraction (XRD) as well as X-ray fluorescence (XRF) [14].

Study of effects of micro- and nanometric-sized glass and gold-alloy fragments on Scanning Electron Microscope (SEM) - Energy-Dispersive X-ray Spectrometry (EDS) microanalysis. Monte Carlo simulations of different kinds of elongated glass fragment demonstrated a strong influence in terms of the fragment size and operational conditions. This work can be used to devise an appropriate and optimised measurement strategy [15].

This work aims to differentiate uranium oxide and halides by using a combination of gamma and X-ray Monte Carlo simulation and estimates the ²³⁵U mass contents. All the samples measured are under the Safeguards Agreement between Egypt and IAEA. The reference NMs samples belong to Key Measurement Point (KMP-E) of location outside facility (ETZ) at Egyptian Nuclear & Radiological Regulatory Authority.

2. Methodology

The main objective for non-destructive assay methods is ²³⁵U mass verification. To measure sample count rate faced by the distance detector "D", it can be given as follows from Eqn.1:

$$C_R = M_5 S_{a5} \epsilon_a \quad \text{Eqn. 1}$$

Where C_R refers to net count rate for sample, M_5 is the ²³⁵U mass in sample, S_{a5} refers to specific activity of 185.7 keV energy line, ϵ_a refers to absolute detector efficiency for sample at 185.7 keV energy line. Absolute efficiency can be computed utilizing MCNP-5, where generated input file relies on the sample certificate in addition to details of detector dimensions used [16].

In the Monte Carlo method, it permits simulation of interaction between energetic electron beam and matter with subsequent production and observation of X-rays characteristic of sample elements [17]. Modeling total emitted X-rays by following ionizations and tracking the X-ray trajectories of these electrons is too computationally required, and many methods have been established to overcome such a problem, reducing the required trajectories number. The software requires many electrons to simulate an X-ray Spectrum with a variance of about 1%.

3. Experimental setup and techniques

3.1. Measurements

In this work, we used 11 samples of different compositions and enrichment values ranging from 0.20% to 4.46% in a solid and powder phase with a mass range from 50 to 200.1 gm. Detailed information on each sample is presented in Table 1.

Table 1: Description of samples utilized in measurements.

Sample ID	Chemical formula	Enrichment Range	The total mass of the sample (g)
UM1	U	0.20087%	75
UC1	U ₃ O ₈	0.31000%	200.1
UC2	U ₃ O ₈	0.71000%	200.1
UC3	U ₃ O ₈	1.94000%	200.1
UC4	U ₃ O ₈	2.95000%	200.1
UC5	U ₃ O ₈	4.46000%	200.1
UH1	UF ₃	0.2, 0.71&2%*	50
UH2	UF ₄	0.2, 0.71&2%*	50
UH3	UCl ₃	0.2, 0.71&2%*	50
UH4	UCl ₄	0.2, 0.71&2%*	50
UH5	UI ₃	0.2, 0.71&2%*	50

*Proposed enrichment for samples

The first detector was coaxial construction gamma spectrometer with Micro-trans-SPEC HPGe detector (ORTEC GEM Series), P-type crystal was used in experimental set-up. Detector crystal exhibited a diameter of 50 mm and a length of 33 mm ($\pm 10\%$) in cryostat cooled by the integrated, low-power, Stirling-cycle cryo-cooler, digital multi-channel analyzer with 8192 channels and digital signal processing data acquisition system PC controlled by MAESTRO software from Ortec. The relative efficiency of system is 40% at 1.33 MeV. The sample was located in front of detector. For all measurements, sample-to-AL cap of detector distance was 15 cm. Table 2, Displays geometry characteristics given by the manufacturer for detector [18]. Figure 1 Detector model diagrams as drawn by MCNP Visual Editor to calculate efficiency.

Table 2: Geometry characteristics provided by the manufacturer for detector.

DETECTOR DIAMETER	50 mm
DETECTOR LENGTH	30 mm, MINIMUM
DETECTOR END RADIUS (I)	8 mm, NOMINAL
HOLE DIAMETER	9 ± 1 mm
HOLE DEPTH	15 mm, MINIMUM
HOLE BOTTOM RADIUS	4 mm, NOMINAL

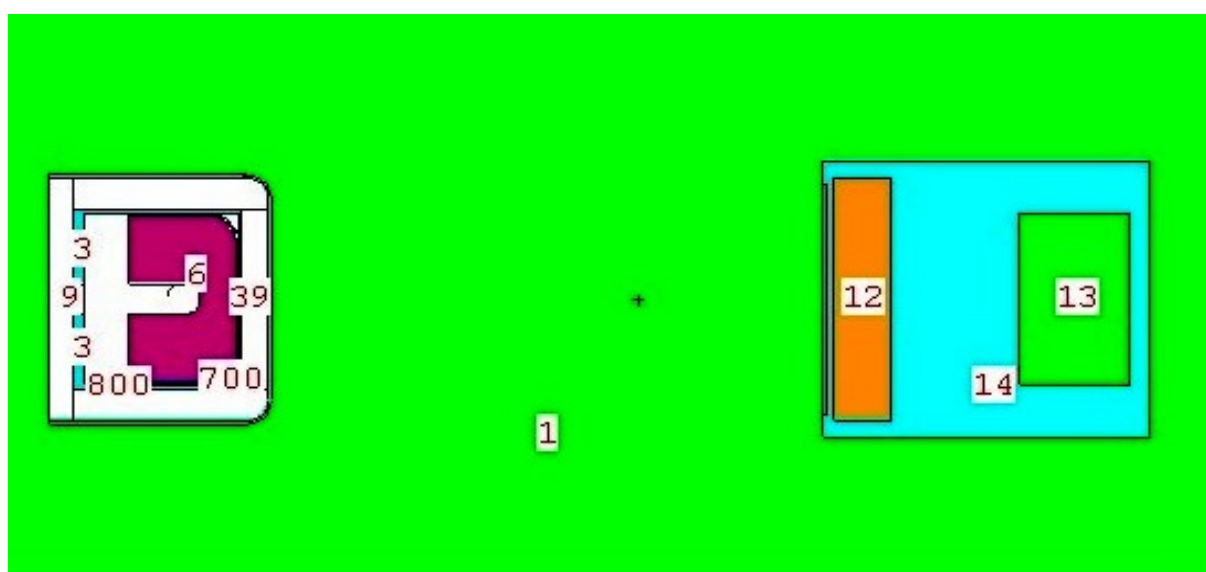


Figure 1: Model of detector as drawn by MCNP visual editor.

The second detector was MCNP work system includes a High Purity Germanium Detector (HPGe) with a Canberra GL0515R model and dynamic area of 540 mm^2 . The height is 1.5 cm, and FWHM is 540 eV at 122 keV. Multi-channel analyzer [Inspector, Model IN2K], for collecting input energy pulses, the detector was adjusted at high voltage (-2500V) to calculate the energy line efficiency and count rates of 185.7 keV for uranium halides at various enrichment. The sample-to-AL cap of detector distances was 25 cm for all calculations [19-21].

3.2. Monte Carlo modeling for the proposed System (Gamma spectrometry)

The General Monte Carlo Code (MCNP-5) has been utilized to calculate absolute efficiency of detector [22]. The Monte Carlo simulation is regarded to be a random number sequence that occurs throughout the simulation. The simulation, relying on the repetition of this sequence, will result in some statistical errors in agreement with the first sequence results [23]. Characteristics as well as specifications of planar and coaxial HPGe detectors and proposed NMs have been modeled [24, 25]. About 20 input files were created for such calculation using 10^8 history with a run time of 25 minutes. The specification of utilized laptop is 2.5 GHz Intel Core i7 processor. The F8 tally card is utilized for determining pulse height of detector. The absolute efficiency of 185.7 keV energy line detector was calculated based on this tally.

3.3. Monte Carlo modeling for the proposed system (X-ray Spectrometry)

Electron interaction with samples has been studied using X-ray simulation software relying on the code developed by NISTMonte. The software is scripted in the Java scripting language. The quantitative analysis using X-ray spectroscopy is performed based on information obtained from electron scattering, X-ray generation, absorption and fluorescence. The simulations were carried out considering conditions similar to experimental data during SEM-EDS analyzes. These conditions, such as primary electron energy, probe size, take-off angle of detector, EDS detector type. The peaks and spectrum of all samples were calculated and used to distinguish the samples' compositions [26, 27].

4. Results and Discussion

4.1. The first detector

An estimate of ^{235}U mass was produced from substitution in Eqn.1, in which count rate was measured experimentally by means of HPGe detector, while absolute full-energy peak efficiency value was calculated by MCNP-5. The declared mass of six uranium standards and estimated isotopic mass content by MCNP code are tilted below in Table 3. As stated by results in Table 3, mass provided by MCNP-5 was consistent with declared mass of U-235 isotope. Mass values were 0.5320, 1.2200, 3.2750, 5.0400, 7.5920 and 0.1572 (g) for 0.31000, 0.71000, 1.94000, 2.95000, 4.46000% and 0.20087% enrichment values, respectively.

Table 3: ^{235}U mass estimated by the described method in comparison with declared value.

Sample ID	Declared Mass (g)	Estimated Isotopic Mass Content M (g) $\pm\sigma_M$	
	^{235}U	^{235}U	Relative Accuracy %
UC1	0.5260	0.5320 \pm 0.0190	1.1407
UC2	1.2050	1.2200 \pm 0.0290	1.2448
UC3	3.2920	3.2750 \pm 0.0310	-0.5164
UC4	5.0060	5.0400 \pm 0.0490	0.6792
UC5	7.5670	7.5920 \pm 0.0980	0.3304
UM1	0.1507	0.1520 \pm 0.0070	0.8626

4.2. The second detector

Tables 4, 5, 6, 7, and 8 demonstrates the efficiency, count rates (C_R) with associated uncertainties (σ_{C_R}) for energy line 185.7 keV at various enrichment values of Uranium Halides ^{235}U masses. It is obvious that counting rate increases and efficiency decreases by increasing sample enrichment.

Table 4: Calculated count rates of energy line 185.7 keV with associated uncertainties for UF3 and ²³⁵U mass estimated.

Enrichment (%)	Efficiency (MCNP)	Cr (s ⁻¹)±(σ _{CR})	Mass of U(g)	U-235 (g)
0.2	1.26471E-05± 0.0022	3.80000E-02±4.32940E-05	40.3400	0.06509
0.71	1.26463E-05± 0.0022	1.35000E-01±15.37010E-05		0.23108
2	1.26443E-05 ±0.0022	3.80000E-01±43.29600E-05		0.65093

Table 5: Calculated count rates of energy line 185.7 keV with associated uncertainties for UF4 and ²³⁵U mass estimated.

Enrichment (%)	Efficiency (MCNP)	Cr (s ⁻¹)±(σ _{CR})	Mass of U(g)	U-235 (g)
0.2	1.42946E-05± 0.0021	3.79000E-02±3.82124E-05	37.90000	0.05745
0.71	1.42935E-05± 0.0021	1.33000E-01±13.37530E-05		0.20109
2	1.42904E-05± 0.0021	3.79000E-01±38.21230E-05		0.57450

Table 6: Calculated count rates of energy line 185.7 keV with associated uncertainties for UCl3 and ²³⁵U mass estimated.

Enrichment (%)	Efficiency (MCNP)	Cr (s ⁻¹)±(σ _{CR})	Mass of U(g)	U-235 (g)
0.2	1.60364E-05± 0.0020	3.53000E-02±3.17805E-05	34.56000	0.04778
0.71	1.60353E-05± 0.0020	1.25000E-01±11.28080E-05		0.16960
2	1.60330E-05± 0.0020	3.53000E-01±31.78040E-05		0.47780

Table 7: Calculated count rates of energy line 185.7 keV with associated uncertainties for UCl4 and ²³⁵U mass estimated

Enrichment (%)	Efficiency (MCNP)	Cr (s ⁻¹)±(σ _{CR})	Mass of U(g)	U-235 (g)
0.2	1.77882E-05± 0.0019	3.22000E-02±2.61203E-05	31.33500	0.03927
0.71	1.77872E-05± 0.0019	1.14000E-01±9.27406E-05		0.13943
2	1.77847E-05± 0.0019	3.22000E-01±26.12010E-05		0.39270

Table 8: Calculated count rates of energy line 185.7 keV with associated uncertainties for UI3 and ²³⁵U mass estimated.

Enrichment (%)	Efficiency(MCNP)	Cr(s ⁻¹)±(σ _{CR})	Mass of U(g)	U-235 (g)
0.2	1.99514E-05± 0.0018	1.36000E-02±0.983808E-05	19.23500	0.01479
0.71	1.99503E-05± 0.0018	4.84000E-02±3.49467E-05		0.05254
2	1.99478E-05± 0.0018	1.36000E-01±9.83743E-05		0.14790

4.3. The X-ray simulation

Figure 2 to Figure 8 represent the peaks of uranium, chlorine, fluorine, iodine and oxygen elements. The proposed samples are uranium metal, triuranium octaoxide, uranium trifluoride, uranium tetrafluoride, uranium trichloride, uranium tetrachloride and uranium triiodide. Table 9, demonstrate Theoretical calculation of uranium oxides and Halides. These samples were theoretically analyzed at this time to get concentration of uranium and oxygen atoms. These samples were simulated using a Si(Li) detector (Dead layer 0.09 μm , Detector area 10 mm^2 , Aluminum window thickness 40 nm and Gold layer thickness=8 nm). Simulation was done at 25 keV.

Element (conc.) (mass %)	Molecular weight	U	O	F	Cl	I
Uranium metal	238.03	100	Nil	Nil	Nil	Nil
U_3O_8	842.08	84.80	15.20	Nil	Nil	Nil
UF_3	295.02	80.68	Nil	19.32	Nil	Nil
UF_4	314.02	75.80	Nil	24.20	Nil	Nil
UCl_3	344.39	69.12	Nil	Nil	30.88	Nil
UCl_4	379.84	62.67	Nil	Nil	37.33	Nil
UI_3	618.74	38.47	Nil	Nil	Nil	61.53

Table 9: Theoretical calculation of uranium oxides and Halides.

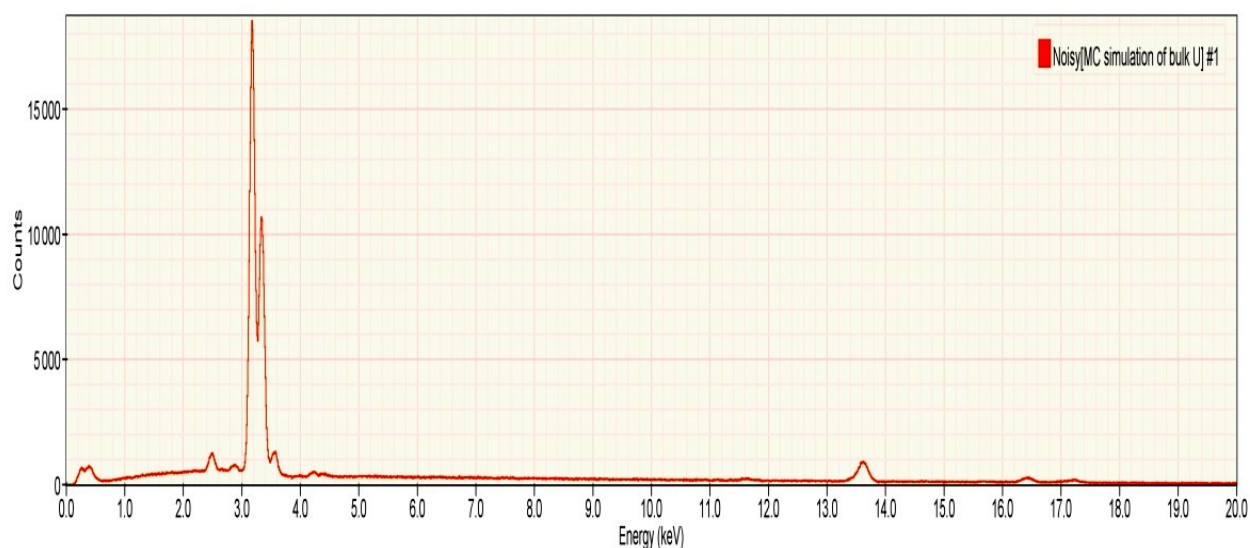


Figure 2: X-ray simulation for uranium metal.

In Figure 2, the X-ray peak for uranium element appears at energy 3.164 keV and 13.612 keV, and its concentration is 100% as it is pure uranium metal.

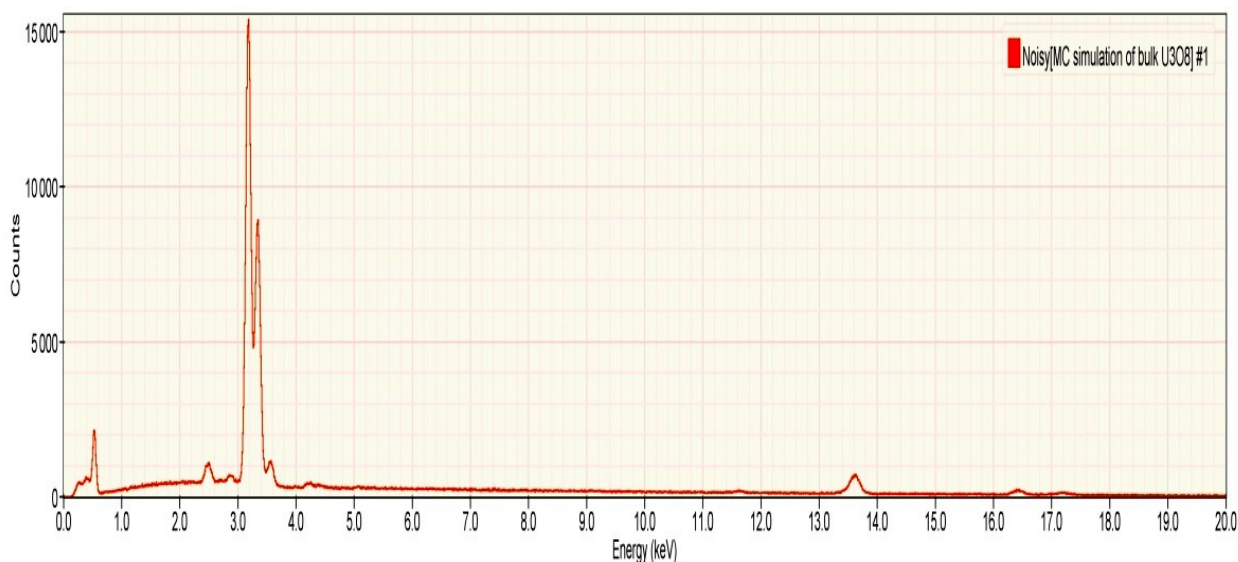


Figure 3: X-ray simulation for triuranium octaoxide.

In [Figure 3](#), the X-ray peaks appear at energy 3.164 keV and 13.612 keV for uranium and 0.525 keV for oxygen, and the concentrations are 84.80% and 15.20%, respectively.

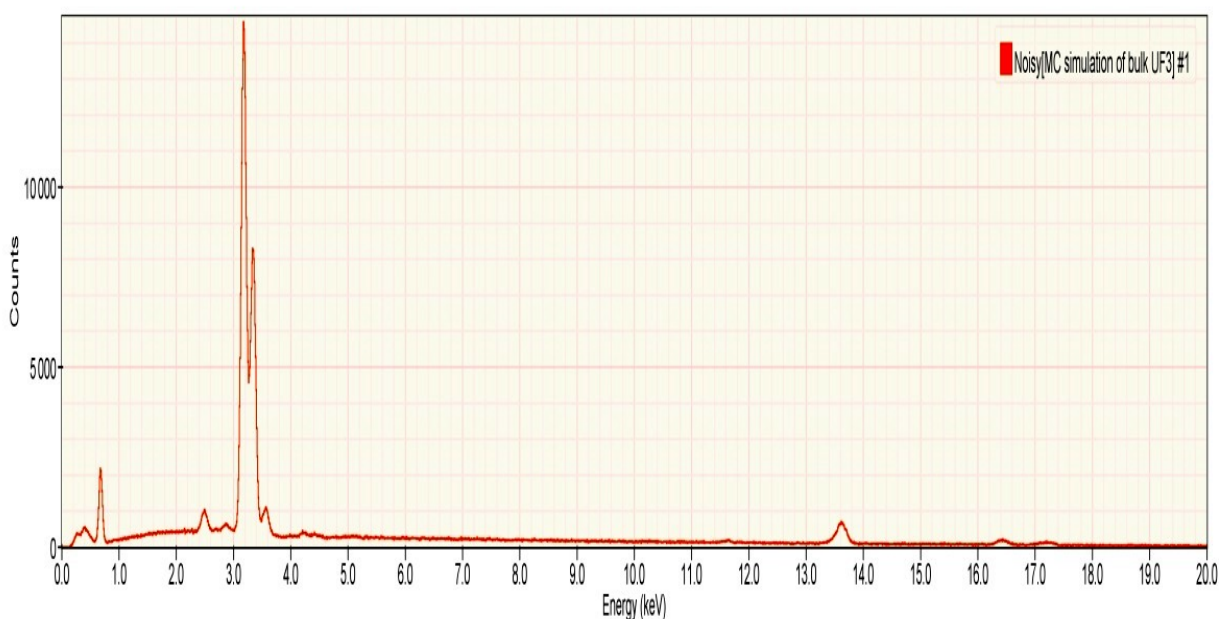


Figure 4: X-ray simulation for uranium trifluoride.

In [Figure 4](#), the X-ray peaks appear at energy 3.164 keV and 13.612 keV for uranium and 0.677 keV for fluorine, and the concentrations are 80.68% and 9.32%, respectively. In [Figure 5](#), the X-ray peaks appear at energy 3.164 keV and 13.612 keV for uranium and 0.677 keV for fluorine, and the concentrations are 75.80%, 24.20%, respectively. It is observed the concentration of uranium in UF_3 is greater than UF_4 due to the difference in number of moles of fluorine between the two chemical formulas.

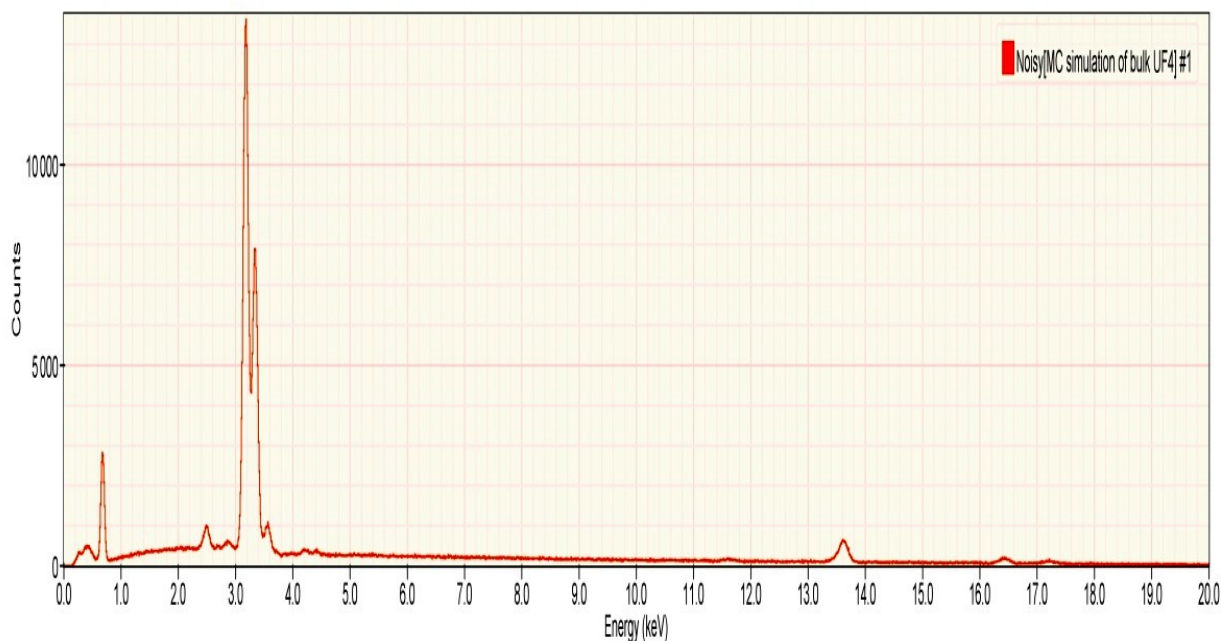


Figure 5: X-ray simulation for uranium tetrafluoride

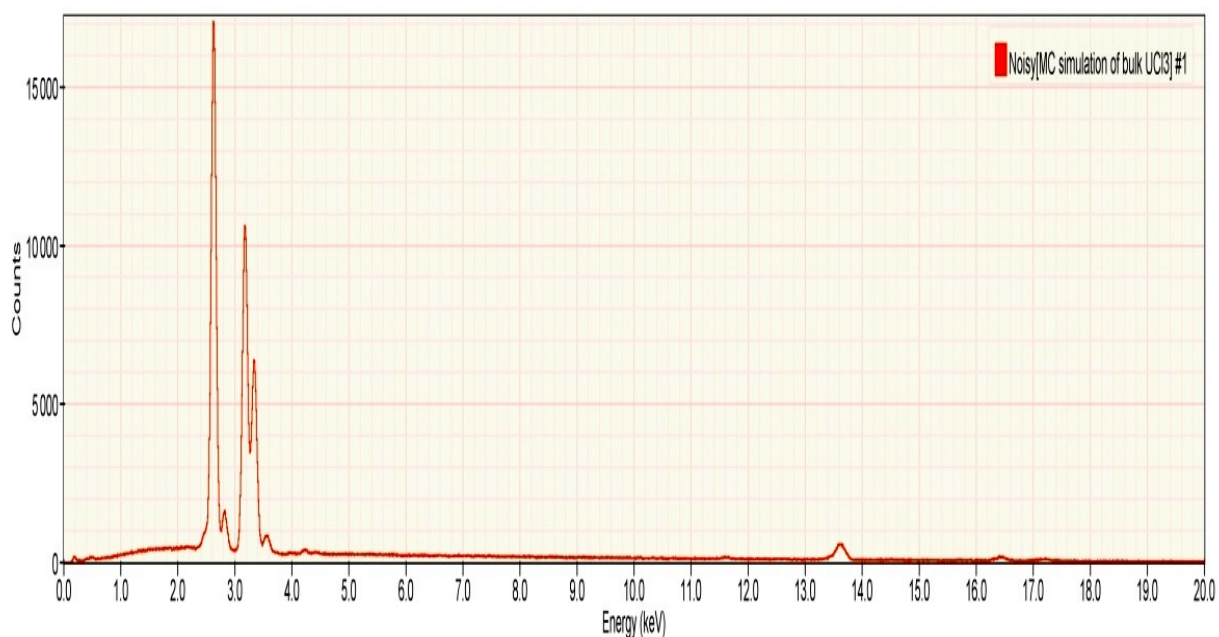


Figure 6: X-ray simulation for uranium trichloride

In [Figure 6](#), the X-ray peaks appear at energy 3.164 keV and 13.612 keV for uranium and 2.621 keV for chlorine, and the concentrations are 69.12% and 30.88%, respectively. In [Figure 7](#), the X-ray peaks appear at energy 3.164 keV and 13.612 keV for uranium and 2.621 keV for chlorine, and the concentrations are 62.67% and 37.33%, respectively. It is observed that uranium concentration in UCl_3 is greater than UCl_4 due to difference in number of chlorine moles between the two chemical formulas.

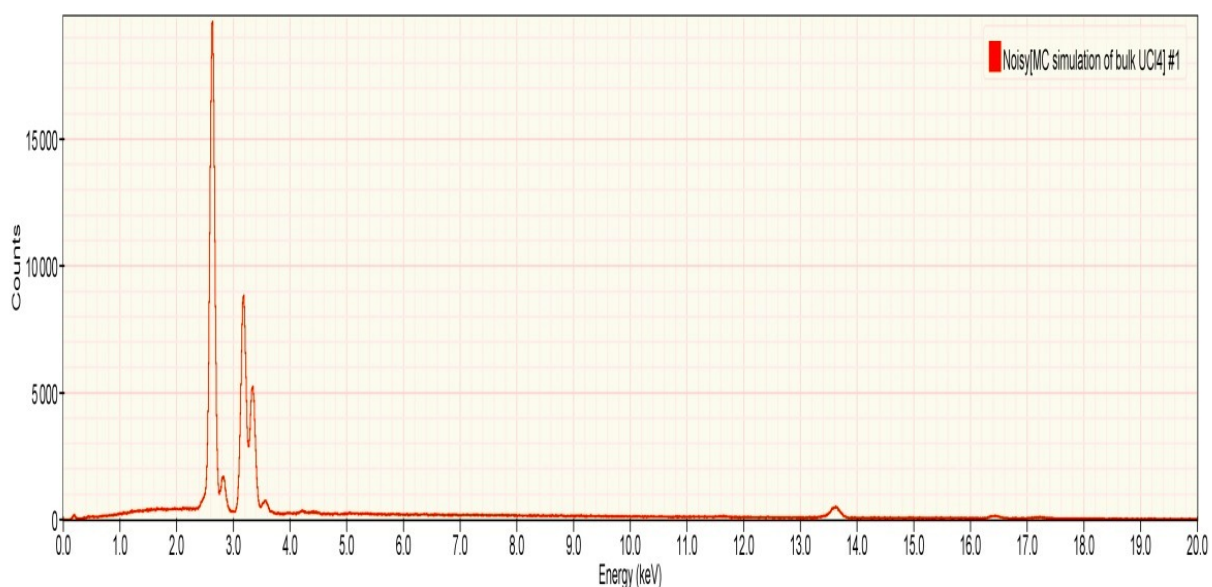


Figure 7: X-ray simulation for uranium tetrachloride

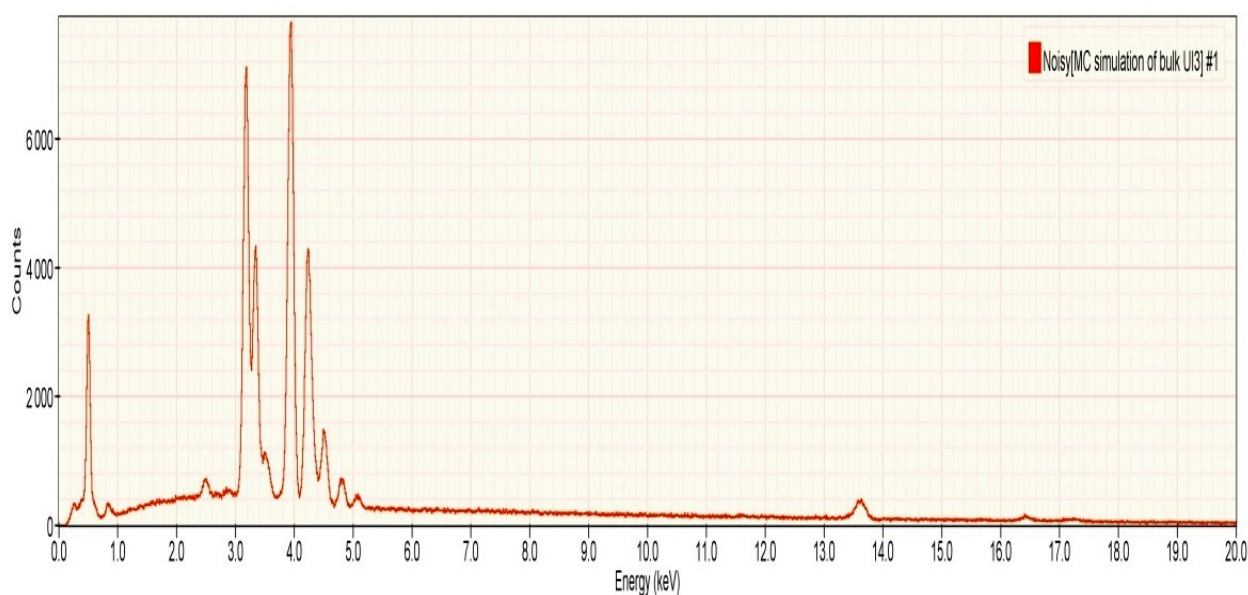


Figure 8: X-ray simulation for uranium triiodide.

In **Figure 8**, the X-ray peaks appear at energy 3.164 keV and 13.612 keV for uranium and 3.937 keV for iodine, and the concentrations are 38.47% and 61.53%, respectively. It is observed UI_3 has the least concentration among studied uranium halides due to the high mass number of iodine.

Conclusion

Verification of different forms of NMs such as Low Enriched Uranium (LEU), Nature Uranium (NU) and Depleted Uranium (DU) is a challenge for the safeguard inspectors. To deal with this challenge, many techniques such as Gamma rays and X-rays spectrometry can be employed. Combination between X-ray and Gamma ray tools can reveal information about the assayed sample like chemical composition

isotopic and isotopic ratio. X-ray tool is useful when the element concentration is needed. Gamma ray tool and MCNP-5 are essential for calculating parameters like U-235 isotope mass. Finally, theoretical and experimental tools can give the analyst a complete view about the qualitative and quantitative information of any NM sample.

References

- [1] N. V. De Castro, and R. J. A. Lévesque, "Photo peak and Double Escape Peak Efficiencies of Germanium Lithium Drift Detectors", *Nuclear Instruments and Methods*, 46 (1967) 325-332. [https://doi.org/10.1016/0029-554X\(67\)90091-2](https://doi.org/10.1016/0029-554X(67)90091-2)
- [2] B. Lal, and K.V.K. Iyengar, "Monte Carlo calculations of gamma ray response characteristics of cylindrical Ge(Li) detectors", *Nuclear Instruments and Methods*, 79 (1970) 19-28. [https://doi.org/10.1016/0029-554X\(70\)90004-2](https://doi.org/10.1016/0029-554X(70)90004-2)
- [3] T. Nakamura, "Monte Carlo calculation of peak efficiencies and response functions of coaxial-type Ge(Li) detectors for disk gamma-ray sources", *Nuclear Instruments and Methods*, 131 (1975) 521-527. [https://doi.org/10.1016/0029-554X\(75\)90444-9](https://doi.org/10.1016/0029-554X(75)90444-9)
- [4] Sunita Kamboja and Bernd Kahn, *Radiation Measurements*, (2003) 371.
- [5] O. Sima, "Application of response functions to make efficient Monte Carlo simulations of germanium detectors", *Applied Radiation and Isotopes*, 68 (2010) 1403-1406. <https://doi.org/10.1016/j.apradiso.2010.01.014>
- [6] P. P. Maleka, and M. Maucec, "Monte Carlo uncertainty analysis of germanium detector response to gamma-rays with energies below 1 MeV", *Nuclear instruments & methods in physics research Section A*, 538 (2005) 631-639. <https://doi.org/10.1016/j.nima.2004.09.012>
- [7] S. Hurtado, M. Garcia-Leon, and R. Garcia-Tenorio, "Monte Carlo simulation of the response of a germanium detector for low-level spectrometry measurements using GEANT4", *Applied Radiation and Isotopes*, 61(2004)139-143. <https://doi.org/10.1016/j.apradiso.2004.03.035>
- [8] R. Berndt, and P. Mortreau, "Monte Carlo modelling of a N-type coaxial high purity germanium detector", *Nuclear Instruments and Methods in Physics Research Section A*, 694 (2012) 341-347. <https://doi.org/10.1016/j.nima.2012.07.006>
- [9] B. Blank, J. Souin, P. Ascher, L. Audirac, G. Cachel, M. Gerbaux, ... and J. C. Thomas, "High-precision efficiency calibration of a high-purity co-axial germanium detector", *Nuclear Instruments and Methods in Physics Research Section A*, 776 (2015)34-44. <https://doi.org/10.1016/j.nima.2014.12.071>
- [10] J. Gasparro, M. Hult, P. N. Johnston, and H. Tagziria, "Monte Carlo modelling of germanium crystals that are tilted and have rounded front edges", *Nuclear Instruments and Methods in Physics Research Section A*, 594 (2008) 196-201.
- [11] S. U. Rehman, S. M. Mirza, N. M. Mirza, and M. T. Siddique, "GEANT4 simulation of photo-peak efficiency of small high purity germanium detectors for nuclear power plant applications", *Annals of Nuclear Energy*, 38 (2011) 112-117. <https://doi.org/10.1016/j.anucene.2010.08.010>
- [12] W. EL-GAMMAL, "Verification of ²³⁵U mass content in nuclear fuel plates by an absolute method", *Nuclear Instruments and Methods in Physics Research Section A*, 570 (2007) 446-453. <https://doi.org/10.1016/j.nima.2006.09.114>
- [13] S. E. Shaban, M. H. Hazzaa, R. A. El-Tayebany, and M. A. Abdalsamia, "Countering distortion scenarios outcome from shaping and the chemical mixing in U₃O₈-Al compact using reliable

model", *Journal of Radiation Research and Applied Sciences*, 13(1) (2020) 88-93. DOI: [10.1080/16878507.2020.1715557](https://doi.org/10.1080/16878507.2020.1715557)

- [14] J. E. Turner, *Atoms, radiation, and radiation protection*. John Wiley & Sons, (2008).
- [15] Daniele Moro, Gianfranco Ulian, Giovanni Valdrè, "Mineral diagnostics: SEM-EDS Monte Carlo strategy for optimised measurements of ultrathin fragments in cultural heritage studies", *Acta IMEKO*, 10(2021) 193-200. http://dx.doi.org/10.21014/acta_imeko.v10i1.832
- [16] Sameh, E. Shaban, M.H. Hazzaa and R.A. El-Tayebany, "Applying Monte Carlo and artificial intelligence techniques for ^{235}U mass prediction in samples with different enrichments", *Nuclear Instruments and Methods in Physics Research Section A*, 916 (2019) 322–326. <https://doi.org/10.1016/j.nima.2018.10.008>
- [17] D. Moro, G. Ulian, and G. Valdrè, "SEM-EDS microanalysis of ultrathin glass and metal fragments: measurement strategy by Monte Carlo simulation in cultural heritage and archaeology", *International journal of conservation science*, (2020) 11.
- [18] W. I. Zidan, "Refining of a Mathematical Model for a HPGe Detector", *Journal of Nuclear and Particle Physics*, 5 (2015) 30-37. DOI: [10.5923/j.jnpp.20150502.02](https://doi.org/10.5923/j.jnpp.20150502.02)
- [19] Canberra Industries, Germanium Detectors, User's manual, USA, (1995).
- [20] Canberra, Detector Specification and Performance Data (HPGe Model GL0515R- 7905SL-5) USA, (1996).
- [21] R. Gunnink, W. D. Ruhter, P. Miller, J. Goerten, M. Swinhoe, H. Wagner... and S. Abousahl, "MGAU: A new analysis code for measuring ^{235}U enrichments in arbitrary samples", (No. UCRL-JC-114713; CONF-940307-13). Lawrence Livermore National Lab., CA (United States) (1994).
- [22] W. El-Gammal, M. El-Nagdy, M. Rizk, S. Shawky, and M. A. Samei, "Verification of nuclear fuel plates by a developed non-destructive assay method", *Nuclear Instruments and Methods in Physics Research Section A*, 553 (2005) 627-638. <https://doi.org/10.1016/j.nima.2005.07.030>
- [23] X-5 Monte Carlo Team, MCNP – A General Monte-Carlo N-Particle Transport Code, Version 5, LA-UR- 03-1987, (2003).
- [24] NBS, Uranium Isotopic Standard Reference Material for Gamma Spectrometry Measurements 969, NBS-111, Gaithersburg, MD 20899, USA, (1985).
- [25] New Brunswick Laboratory (NBL), uranium assay standard, CRM -115, (2002).
- [26] R. L. Myklebust, D. E. Newbury, and H. Yakowitz, "NBS Monte Carlo electron trajectory calculation program", *NBS Special Publication*, 460 (1976) 105-125.
- [27] N. W. Ritchie, "A new Monte Carlo application for complex sample geometries". *Surface and Interface Analysis*, 37 (2005) 1006-1011. <https://doi.org/10.1002/sia.2093>

(2021); <http://www.jmaterenvironsci.com>